

# Deviation From Normative Whole Brain and Deep Gray Matter Growth in Children With MOGAD, MS, and Monophasic Seronegative Demyelination

Giulia Fadda, MD, Alonso Cardenas de la Parra, PhD, Julia O'Mahony, PhD, Patrick Waters, PhD, E. Ann Yeh, MD, Amit Bar-Or, MD, Ruth Ann Marrie, MD, PhD, Sridar Narayanan, PhD, Douglas L. Arnold, MD, D. Louis Collins, PhD, and Brenda Banwell, MD, for the Canadian Pediatric Demyelinating Disease Network

## Correspondence

Dr. Banwell  
banwellb@email.chop.edu

*Neurology*® 2023;101:e425-e437. doi:10.1212/WNL.0000000000207429

## Abstract

### Background and Objectives

Pediatric-acquired demyelination of the CNS associated with antibodies directed against myelin oligodendrocyte glycoprotein (MOG; MOG antibody-associated disease [MOGAD]) occurs as a monophasic or relapsing disease and with variable but often extensive T2 lesions in the brain. The impact of MOGAD on brain growth during maturation is unknown. We quantified the effect of pediatric MOGAD on brain growth trajectories and compared this with the growth trajectories of age-matched and sex-matched healthy children and children with multiple sclerosis (MS, a chronic relapsing disease known to lead to failure of normal brain growth and to loss of brain volume) and monophasic seronegative demyelination.

### Methods

We included children enrolled at incident attack in the prospective longitudinal Canadian Pediatric Demyelinating Disease Study who were recruited at the 3 largest enrollment sites, underwent research brain MRI scans, and were tested for serum MOG-IgG. Children seropositive for MOG-IgG were diagnosed with MOGAD. MS was diagnosed per the 2017 McDonald criteria. Monophasic seronegative demyelination was confirmed in children with no clinical or MRI evidence of recurrent demyelination and negative results for MOG-IgG and aquaporin-4-IgG. Whole and regional brain volumes were computed through symmetric nonlinear registration to templates. We computed age-normalized and sex-normalized *z* scores for brain volume using a normative dataset of 813 brain MRI scans obtained from typically developing children and used mixed-effect models to assess potential deviation from brain growth trajectories.

### Results

We assessed brain volumes of 46 children with MOGAD, 26 with MS, and 51 with monophasic seronegative demyelinating syndrome. Children with MOGAD exhibited delayed ( $p < 0.001$ ) age-expected and sex-expected growth of thalamus, caudate, and globus pallidus, normalized for the whole brain volume. Divergence from expected growth was particularly pronounced in the first year postonset and was detected even in children with monophasic MOGAD. Thalamic volume abnormalities were less pronounced in children with MOGAD compared with those in children with MS.

From the Department of Medicine (G.F.), University of Ottawa, Ottawa Hospital Research Institute; Montreal Neurological Institute (A.C.P., S.N., D.L.A., D.L.C.), McGill University, Quebec; Department of Community Health Sciences (J.O.M., R.A.M.), Max Rady College of Medicine, Rady Faculty of Health Sciences, University of Manitoba, Winnipeg, Canada; Nuffield Department of Clinical Neurosciences (P.W.), John Radcliffe Hospital, University of Oxford, United Kingdom; Department of Pediatrics (E.A.Y.), University of Toronto, Ontario, Canada; Center for Neuroinflammation and Neurotherapeutics (A.B.-O.), and Department of Neurology, Perelman School of Medicine, University of Pennsylvania, Philadelphia; Department of Internal Medicine (R.A.M.), Max Rady College of Medicine, Rady Faculty of Health Sciences, University of Manitoba, Winnipeg, Canada; and Division of Child Neurology (B.B.), Department of Neurology, The Children's Hospital of Philadelphia, Perelman School of Medicine, University of Pennsylvania.

Go to [Neurology.org/N](https://www.neurology.org/N) for full disclosures. Funding information and disclosures deemed relevant by the authors, if any, are provided at the end of the article.

Canadian Pediatric Demyelinating Disease Network coinvestigators are listed in the appendix at the end of the article.

## Glossary

**ADEM** = acute disseminated encephalomyelitis; **ADS** = acquired demyelinating syndromes; **CAL** = Children's Hospital in Calgary; **CHOP** = Children's Hospital of Philadelphia; **CPDDS** = Canadian Pediatric Demyelinating Disease Study; **EDSS** = Expanded Disability Status Scale; **ETL** = echo train length; **HSC** = Hospital for Sick Children; **NIHPD** = NIH Study of Normal Brain Development; **ON** = optic neuritis; **PNC** = Philadelphia Neurodevelopmental Cohort; **POMS** = pediatric-onset multiple sclerosis; **TM** = transverse myelitis.

## Discussion

The onset of MOGAD during childhood adversely affects the expected trajectory of growth of deep gray matter structures, with accelerated changes in the months after an acute attack. Further studies are required to better determine the relative impact of monophasic vs relapsing MOGAD and whether relapsing MOGAD with attacks isolated to the optic nerves or spinal cord affects brain volume over time.

The demyelinating disease associated with antibodies directed against myelin oligodendrocyte glycoprotein (MOG; MOG antibody-associated disease [MOGAD]) manifests with either a monophasic or a relapsing course and with heterogeneous clinical attack phenotypes.<sup>1,2</sup> MOGAD accounts for approximately one-third of all causes of acquired demyelinating syndromes (ADS) in children, follows a monophasic course in most individuals, and has an overall favorable clinical outcome regarding recovery from incident attack.<sup>3,4</sup> Brain lesion volumes and distributions vary across different clinical presentations, with absent brain lesions in some children with optic neuritis (ON) or transverse myelitis (TM), multifocal large ill-defined lesions involving white matter and both cortical and deep gray matter in children with acute disseminated encephalomyelitis (ADEM), and a variable pattern of lesions in the cortex, supratentorial and infratentorial white matter and deep gray nuclei in children with other presentations. While pediatric MOGAD shares many clinical attack features seen in pediatric-onset multiple sclerosis (POMS), there are key distinctions. Unlike POMS, where multifocal brain lesions at onset and accrual of new lesions over time are a hallmark of the disease, with clear disruption of maturational brain growth,<sup>5-8</sup> the variable extent of brain involvement in pediatric MOGAD and the monophasic course without new lesions over time in many patients may have a very different impact of brain health. Furthermore, most children with MOGAD recover well from attacks, have a low likelihood of neurologic disability (at least in the first 4 years post-onset),<sup>3,9-11</sup> and do not seem to accrue neurologic disability independent of relapses.<sup>12</sup> It might then be hypothesized that MOGAD would have a less negative impact age-expected brain growth.

Monophasic ADS also occur in the absence of MOG-IgG (or other identifiable antibodies), termed “seronegative mono-ADS.” We have previously published that even monophasic demyelination of the CNS during childhood has the potential to negatively affect brain tissue integrity, as measured by brain growth trajectories and diffusion tensor imaging.<sup>6,13</sup>

Owing to the relatively recent availability of high-quality MOG-IgG assays<sup>14</sup> that enable ascertainment of a MOGAD diagnosis, long-term outcome data for confirmed MOGAD are limited. Studies of brain volume in MOGAD are also scarce and limited by cross-sectional design.<sup>15-19</sup> No study to date has investigated the trajectory of brain growth in children with MOGAD.

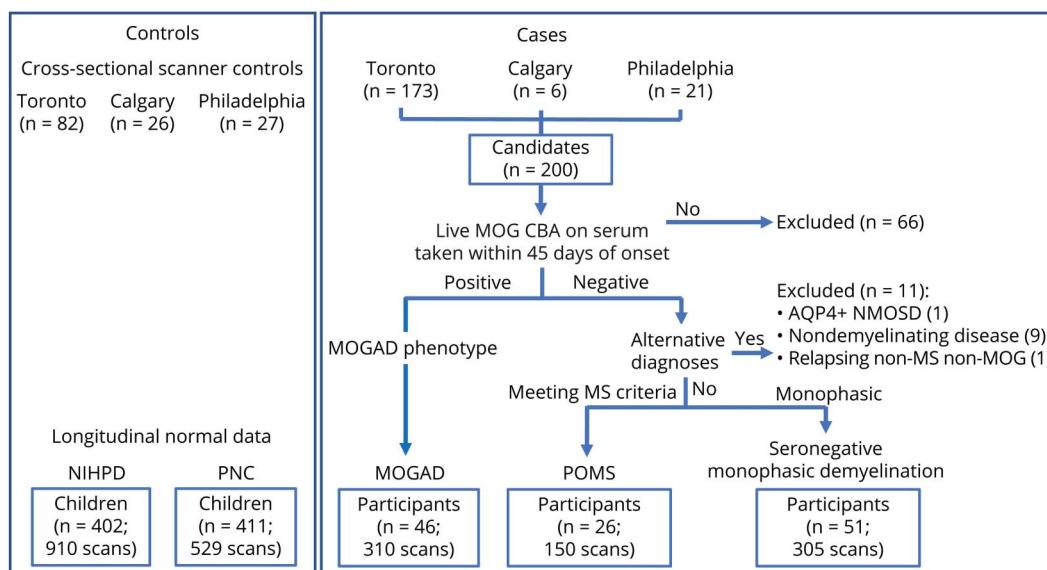
Leveraging a prospective collection of serial research brain MRIs, we first assessed the growth trajectories of the whole brain and deep gray matter structures in children with MOGAD, compared with age-normalized and sex-normalized data. We then evaluated whether patients with MOGAD with ON (and no brain lesions) differed from patients with MOGAD presenting with ADEM, to evaluate whether the presence of brain lesions at presentation could affect brain volume outcome. Finally, we compared the growth trajectories in children with MOGAD with those of children with POMS and seronegative mono-ADS.

## Methods

### Participants

The study cohort was identified from the participants of the Canadian Pediatric Demyelinating Disease Study (CPDDS). Between 2004 and 2017, this study enrolled individuals younger than 16 years (from 2004 to 2014) and younger than 18 years (from 2014 to 2017) who presented with the first clinical episode of acquired CNS demyelinating syndromes (ADS) at any of the participating sites (23 pediatric centers in Canada and 1 in the United States).<sup>20</sup> Each site collected serial MRI scans from children with ADS. To reduce the variability of MRI metrics related to the use of different scanners, for this study, we included participants who (1) underwent brain MRI research scans at the 3 largest CPDDS sites (the Hospital for Sick Children (HSC) in Toronto, the Alberta Children's Hospital in Calgary (CAL), and the Children's Hospital of Philadelphia (CHOP)); (2) had serum anti-MOG antibody testing performed; (3) in case of anti-MOG antibody seronegative result, had the first available sample obtained no later

**Figure 1** Flowchart of Patient Recruitment



than 45 days from initial presentation (to minimize the possibility of early conversion to seronegative status); and (4) had diagnosis of monophasic or relapsing MOGAD (MOG-IgG positive serology as confirmed by a live cell-based assay, measured at a single site previously described,<sup>3</sup> and phenotype consistent with typical MOGAD), MS,<sup>21</sup> or seronegative mono-ADS (as determined by the absence of clinical or MRI evidence of relapses or new lesions over follow-up and negative MOG-IgG) (Figure 1). For each study participant, demographic and clinical information was collected. Disability outcome was extrapolated from a standardized clinical examination, collected at each study visit, to create an estimated Expanded Disability Status Scale (EDSS) score.<sup>22</sup>

We used normative brain MRI data obtained from 402 children (910 total longitudinal scans) from the NIH Study of Normal Brain Development (NIHPD)<sup>23</sup> and 411 children (529 total longitudinal scans) from the Philadelphia Neurodevelopmental Cohort (PNC)<sup>24</sup> to establish normative brain volume vs age trajectories, separated by sex. MRI scans were also acquired at a single time point from typically developing healthy children (n = 135) with a history showing negative results for neurologic, medical, or psychiatric diseases, enrolled at the 3 main CPDDS sites of Calgary, Toronto, and Philadelphia. As per our prior work,<sup>7,25,26</sup> data from these local controls acquired on the same scanners of our patient population allowed us to exclude the presence of scanner-related differences between the cohorts of healthy children from the CPDDS, NIHPD, and PNC studies.

### Standard Protocol Approvals, Registrations, and Patient Consents

The study was approved by the research ethics boards of all participating institutions. Guardians and participants provided written informed assent/consent.

### Anti-MOG Antibody Testing

Serum samples collected at clinical onset and subsequent serial study visits were archived. Samples were batch shipped to the Autoimmune Neurology diagnostic laboratory in Oxford University, and analyzed using a live cell-based assay as previously described,<sup>3</sup> blinded to clinical details.

### MRI Acquisition

Participants from the CPDDS followed at HSC were scanned using either a 1.5T GE Signa Excite scanner with a sagittal, 3D T1-weighted (T1w), RF-spoiled, gradient-recalled echo sequence (TR = 22 msec, TE = 8 msec, flip angle = 30°, voxel size = 0.98 × 0.98 × 1.5 mm, 110 partitions) and an axial 2D multislice dual-echo proton density-weighted (PDw)/T2w fast spin-echo sequence (TR = 3,500 msec, TE1/TE2 = 15/63 msec, echo train length [ETL] = 8, voxel size = 0.98 × 0.98 × 2 mm, 85 slices, no gap) or a 3.0T Siemens TIM Trio scanner with an axial 3D T1w MPRAGE sequence (TR = 1810 msec, TE = 3.51 msec, TI = 1,100 msec, flip angle = 9°, voxel size = 0.94 × 0.94 × 1 mm), a PDw fast spin-echo sequence (TR = 2,200 msec, TE = 10 msec, ETL = 4, voxel size 1 × 1 × 3 mm, 60 slices, no gap), and a T2w spin-echo sequence (TR = 4,500 msec, TE = 84 msec, ETL = 11, voxel size 1 × 1 × 3 mm, 60 slices, no gap). CPDDS participants at the Calgary site were scanned using a 1.5T Siemens Avanto scanner with a sagittal 3D T1w FLASH sequence (TR = 22 msec, TE = 8 msec, flip angle = 30°, voxel size 0.98 × 0.98 × 1.5 mm, 128 partitions) and an axial PDw/T2w fast spin-echo sequence (TR = 3,500 msec, TE1/TE2 = 10/73 msec, ETL = 7, voxel size = 0.98 × 0.98 × 2 mm, 82 slices, no gap). Participants from the CPDDS recruited at CHOP were scanned using a 3.0T Siemens Verio scanner with an axial 3D T1w MPRAGE sequence (TR = 1910 msec, TE = 2.88 msec, TI = 1,050, flip angle = 9°, voxel size = 0.94 × 0.94 × 1 mm) a PDw fast spin-echo sequence (TR = 2,200 msec, TE = 10 msec, ETL = 4, voxel size 1 × 1 × 3 mm, 60 slices, no gap) and a T2w spin-echo sequence

(TR = 4,500 msec, TE = 84 msec, ETL = 11, voxel size 1 × 1 × 3 mm, 60 slices, no gap).

The NIHPD HCs were scanned at 6 centers on Philips, GE, or Siemens (Erlangen, Germany) 1.5T scanners. All acquisitions included a 3D T1w RF-spoiled gradient-recalled echo (1-mm thick sagittal partitions, TR = 22–25 msec, TE = 10–11 msec, excitation pulse angle 30°, voxel size = 0.98 × 0.98 × 1.5 mm). The PNC HCs were scanned at a single study center using a 3.0T Siemens TIM Trio and included a whole-brain, 3D T1w MPRAGE sequence (TR = 1810 msec, TE = 3.51 msec, TI = 1,100 msec, flip angle = 9°, voxel size = 0.94 × 0.94 × 1 mm).

## Image Processing

The longitudinal automatic image processing pipeline developed for our prior work (Aubert-Broche et al., 2013) was adapted for this dataset. In short, T1w image processing included (1) denoising,<sup>27</sup> (2) intensity inhomogeneity correction,<sup>28</sup> (3) intensity normalization to a range of 0–100, (4) stereotaxic registration using a 9-parameter transformation,<sup>29</sup> (5) brain extraction,<sup>30</sup> and (6) symmetric (SyN) nonlinear registration<sup>31</sup> to a labeled unbiased stereotaxic template<sup>32</sup> for segmentation. Volumes for whole brain, thalamus, putamen, caudate, and globus pallidus were calculated. The right and left volumes of gray matter structures were averaged for analysis and normalized by the whole brain volume.

## Z Scores Computation

Structure volume z scores were used to normalize for the effect of healthy age-related growth and sex in a pediatric population. Z scores for each brain structure were computed by subtracting the mean and dividing by the SD (estimated from the variance-covariance matrix of the fixed effects and the residual variance of the random effects) using the age and sex for the specific participant. The mixed-effects model included a bias term to correct for site-related differences in scanning parameters and field strength between our normative dataset and the 3 acquisition sites of the CPDDS. Full details about this methodology and its validation can be found in previous publications.<sup>26,33</sup>

## Statistical Analysis

The Z scores of brain and gray matter structures were initially compared cross-sectionally at baseline between children with MOGAD, POMS, and seronegative mono-ADS using the Mann-Whitney *U* test.

The trajectories of normalized volumes were assessed using linear mixed-effect models in children with MOGAD, POMS, and seronegative mono-ADS with the following formula:

$$Z_{ij} = b_0 + y_{0i} + b_1 \text{ Disease Duration}_{ij} + \varepsilon_{ij}$$

where  $Z_{ij}$  is the value of the volume z score for time point  $j$  of participant  $i$ ,  $\text{Disease Duration}_{ij}$  is the time since first demyelinating event for time point  $j$  of participant  $i$ ,  $b_0$  is the model intercept,  $b_1$  is the model slope,  $y_{0i}$  is the coefficient specific for participant  $i$ , and  $\varepsilon_{ij}$  is an error term. To assess

whether abnormal growth could be detected after a single demyelinating attack, we performed a sensitivity analysis restricted to children with monophasic MOGAD. To exclude a disproportional contribution of participants with longer follow-up to the overall growth trajectory, we performed an additional analysis restricted to the first 5 years from presentation (i.e., the median length of follow-up in children with MOGAD).

The comparison between different diagnostic groups (MOGAD, MS, and mono-ADS) and between distinct MOGAD subgroups (that is, participants with MOGAD presenting with ADEM vs ON and those with brain lesions vs without brain MRI lesions at presentation) was computed through the inclusion of an additional *group* term to the models as follows:

$$Z_{ij} = b_0 + y_{0i} + b_1 \text{ Disease Duration}_{ij} + b_2 \text{ group}_i + b_3 \text{ group}_i \\ * \text{ Disease Duration}_{ij} + \varepsilon_{ij}$$

Finally, we binned the volume measurements into 2 groups: those acquired at early time points (up to 1 year from presentation) vs later time points (greater than 1 year from onset) and compared the trajectories between these 2 disease stages through the inclusion of a *phase* term:

$$Z_{ij} = b_0 + y_{0i} + b_1 \text{ Disease Duration}_{ij} + b_2 \text{ phase} + b_3 \text{ phase} \\ * \text{ Disease Duration}_{ij} + \varepsilon_{ij}$$

To account for the presence of multiple comparisons, *p* values < 0.001 were considered statistically significant. The analyses were performed using the statsmodels library<sup>34</sup> in Python version 3.6.5 (Python Software Foundation).

## Data Availability

Anonymized derived data used for this article will be made available by request from qualified investigators.

## Results

### Participants

A total of 46 children with MOGAD, 26 with POMS, and 51 with seronegative mono-ADS met the inclusion criteria (Figure 1). Clinical and demographic features of the study cohort are reported in Table 1.

Brain lesions were observed in 76% of children with MOGAD on MRI scans acquired at onset, whereas all children with MS had brain lesions, as did half of the children with seronegative mono-ADS. Median disability scores in proximity to the presenting attack (median 8 days from symptoms onset, IQR 4–16) were higher in participants with seronegative mono-ADS (EDSS 6.5, IQR 3.0–7.5) compared with those with MOGAD (EDSS 3.0, IQR 1.0–6.5) and MS (EDSS 3.0, IQR 2.0–4.5). At the last clinical follow-up (after a median of 6.8 years from first presentation), scores were low across diagnostic groups, with most children with MOGAD only



**Table 1** Demographic and Clinical Characteristics of the Study Cohort

	MOGAD	MS	Mono-ADS
Participants	46	26	51
Age at presentation (median [IQR])	8.34 (5.71 to 11.53)	14.64 (13.55 to 15.61)	11.83 (8.53 to 13.44)
Female, n (%)	28 (61)	17 (65)	24 (47)
Presenting phenotype, n (%)			
ADEM	15 (33)	0 (0)	8 (16)
Monofocal ON	21 (46)	6 (23)	15 (29)
Monofocal TM	2 (4)	1 (4)	17 (33)
ON + TM	3 (7)	0 (0)	1 (2)
Other	5 (11)	19 (73)	10 (20)
Brain lesion at presentation	35 (76)	26 (100)	26 (51)
Thalamic lesions	17 (37)	6 (23)	7 (14)
Basal ganglia lesions	11 (24)	3 (12)	8 (16)
Clinical relapses	9 (20)	14 (54)	0 (0)
Time from presentation to last clinical follow-up (y) (median [IQR])	7.29 (6.20 to 9.11)	4.84 (3.11 to 6.33)	6.27 (5.01 to 8.97)
EDSS at last clinical follow-up (median [IQR])	1.0 (0.0 to 1.5)	1.5 (1.0 to 2.0)	1.0 (0.0 to 2.25)
Time from presentation to first MRI scan analyzed (d) (median [IQR])	25.57 (10.96 to 184.45)	34.69 (7.30 to 51.13)	10.96 (7.30 to 96.79)
Time from presentation to last MRI scan analyzed (y) (median [IQR])	5.09 (4.00 to 7.04)	4.44 (2.30 to 6.30)	4.09 (3.04 to 6.00)
No. of scans/participant (median [IQR])	7 (5 to 8)	6 (3.5 to 8)	7 (4 to 8)
Baseline brain volume Z score (median [IQR])	-0.25 (-0.80 to 0.30)	-0.15 (-0.95 to 0.34)	-0.32 (-0.90 to 0.38)
Baseline normalized thalamic volume z score (median [IQR])	-0.55 (-1.07 to -0.15)	-0.70 (-1.26 to 0.08)	-0.25 (-1.00 to 0.35)

Abbreviations: ADEM = acute disseminated encephalomyelitis; ON = optic neuritis; TM = transverse myelitis. Data are reported as n (%) or as median (IQR).

exhibiting mild abnormalities on neurologic examination (median EDSS 1, IQR 0–1.5, Table 1).

### Cross-sectional Comparison of Baseline Whole Brain and Deep Gray Matter Structure Volumes

The Z scores (relative to age-matched and sex-matched controls) of whole brain and deep gray matter structures were assessed cross-sectionally in local controls (scanned at the same machine as the patient population) and at the first available time point for the study participants. The first research scans were obtained after a median (IQR) days from incident clinical presentation of 27 (11–184) in children with MOGAD, 35 (7–51) days in children with POMS, and 11 (7–97) days in children with seronegative mono-ADS.

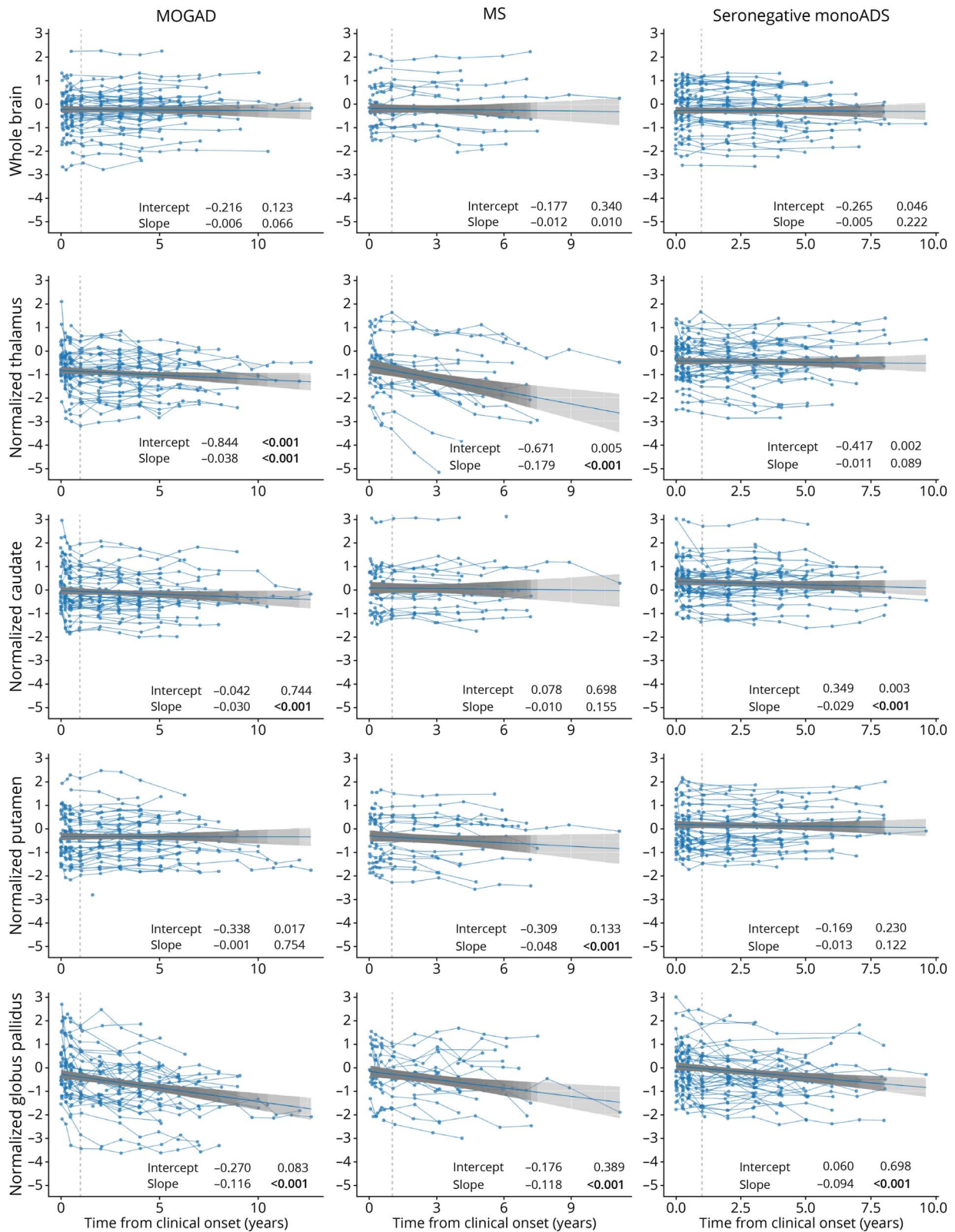
The volume z scores of local controls were not significantly different from those in the healthy children of the NIHPD and PNC studies (which constituted the normative dataset), confirming that results from the study scanners were comparable with data from the larger normative datasets (eFigure 1, [links.lww.com/WNL/C857](https://links.lww.com/WNL/C857)). Baseline Z scores of

thalamus (normalized for total brain volume) were reduced in MOGAD ( $p < 0.0001$ ), while none of the other structures were different from controls at baseline in children with MOGAD (whole brain  $p = 0.06$ , caudate  $p = 0.43$ , putamen  $p = 0.03$ , and globus pallidus  $p = 0.52$ ) nor in any of the other patient groups (eFigure 1).

### Brain Growth Trajectories in Children With MOGAD

The z-scored volume trajectories of whole brain and normalized deep gray matter structures of children with MOGAD, measured over a median of 5.1 years (range 0.5–12.4), are reported in Figure 2. No significant differences from typically developing children were observed in whole brain volume at presentation (intercept) or over time (slope) (Table 2). By contrast, thalamic volume normalized to whole brain volume was smaller during first assessment (negative intercept) and continued to diverge from the expected trajectory of growth (negative slope) over time. Statistically significant negative slopes were observed also for the z scores of normalized caudate and the globus pallidus volumes.

**Figure 2** Growth Trajectories in Children With MOGAD, MS, and Seronegative Mono-ADS



Trajectories of Z scores over time and model fits are plotted for each diagnostic group (from left to right: MOGAD, MS, and seronegative mono-ADS) and for each structure (from top to bottom: whole brain, normalized thalamus, normalized caudate, normalized putamen, and normalized globus pallidus). The vertical dashed line marks 1 year from clinical presentation. The solid blue lines indicate the fitted values of the linear mixed-effect model, while the gray shaded area indicates 95% CI. The model coefficients for the comparisons between groups are reported in Table 2. NIHPD = NIH Study of Normal Brain Development; MOGAD = MOG antibody-associated disease; PNC = Philadelphia Neurodevelopmental Cohort; POMS = pediatric-onset multiple sclerosis.

**Table 2** Z Score Trajectories in Children With MOGAD and Comparison With MS and Seronegative Mono-ADS Groups

	MOGAD vs normal trajectories		MOGAD vs MS		MOGAD vs monoADS	
	Coef. (std.err.)	p Value	Coef. (std.err.)	p Value	Coef. (std.err.)	p Value
<b>Whole brain</b>						
Intercept	-0.216 (0.140)	0.123	0.039 (0.232)	0.868	-0.049 (0.193)	0.798
Slope	-0.006 (0.003)	0.066	-0.007 (0.006)	0.253	0.001 (0.005)	0.868
<b>Normalized thalamus</b>						
Intercept	-0.844 (0.127)	<b>&lt;0.001</b>	0.173 (0.241)	0.473	0.426 (0.200)	0.033
Slope	-0.038 (0.008)	<b>&lt;0.001</b>	-0.141 (0.014)	<b>&lt;0.001</b>	0.027 (0.011)	0.018
<b>Normalized caudate</b>						
Intercept	-0.042 (0.129)	0.744	0.119 (0.219)	0.587	0.391 (0.182)	0.032
Slope	-0.030 (0.006)	<b>&lt;0.001</b>	0.020 (0.011)	0.078	0.001 (0.009)	0.896
<b>Normalized putamen</b>						
Intercept	-0.338 (0.141)	0.017	0.026 (0.244)	0.914	0.510 (0.203)	0.012
Slope	-0.001 (0.004)	0.754	-0.047 (0.011)	<b>&lt;0.001</b>	-0.012 (0.009)	0.151
<b>Normalized globus pallidus</b>						
Intercept	-0.270 (0.156)	0.083	0.094 (0.263)	0.720	0.329 (0.218)	0.132
Slope	-0.116 (0.010)	<b>&lt;0.001</b>	-0.002 (0.018)	0.924	0.022 (0.015)	0.145

These abnormal trajectories were confirmed in the analysis restricted to the first 5 years from presentation (eTable 1, [links.lww.com/WNL/C858](https://links.lww.com/WNL/C858)).

The z-scores of thalamus, caudate, and globus pallidus volumes in children with MOGAD showed a steeper divergence from normality in the first year after presentation, followed by a slower progressive divergence over the subsequent follow-up (Table 3). The divergence from expected growth of normalized thalamus, caudate, and putamen remained significant when the analysis was restricted to the 37 children with monophasic MOGAD (15 of whom presented with ADEM, 13 with monofocal ON, 5 with myelitis, 2 with ON + TM, and 2 with other phenotypes, Figure 3).

### Comparison of Trajectories Between Children With MOGAD, MS, and Seronegative Mono-ADS

Participants with POMS had a greater divergence over time from age-expected growth trajectories of normalized thalamus and putamen compared with those with MOGAD, while no significant difference was detected in the intercept or slope for the whole brain, globus pallidus, or caudate (Figure 2, Table 2). A direct comparison between the growth trajectories during the first year from presentation showed a more pronounced divergence from normative growth of the caudate in children with MOGAD compared with those with MS, while more severe deviation from normal was observed during the subsequent follow-up for the thalamus and globus pallidus among patients with MS (eTable 2, [links.lww.com/WNL/C858](https://links.lww.com/WNL/C858)). The

comparison of the growth trajectories between children with MOGAD and seronegative mono-ADS did not show significant differences.

### Brain Growth Trajectories in Children With MOGAD With and Without Brain Lesions at Presentation

Findings similar to the ones observed in the whole MOGAD cohort (smaller normalized thalamic volume at onset and negative slopes for normalized thalamus, caudate, and globus pallidus) were also observed in the analysis restricted to the 34 children with MOGAD who had brain lesions at onset (14 of whom presented with ADEM, Table 4 and eFigure 2, [links.lww.com/WNL/C857](https://links.lww.com/WNL/C857)).

However, when considering the 11 children with normal brain MRI at onset (10 of whom presented with monofocal ON and 1 with simultaneous ON and myelitis), only the trajectory of normalized globus pallidus was significantly divergent from normal, although the small number of children in this group limited power. Directly comparing the results between patients with MOGAD with and without brain lesions did not reveal statistically significant differences between groups (Table 4). Of note, only 1 of the 12 children without brain lesions at presentation developed new brain lesions at 3 months of follow-up and continued to have stable MRI findings for the subsequent 11 years. Of the 34 children with abnormal brain MRI at presentation, 8 acquired new lesions over follow-up.

**Table 3** Z Scores for Early vs Late Trajectory in MOGAD

	First year postonset		After first year FU		First year vs late FU	
	Coef.	p Value	Coef.	p Value	Coef.	p Value
<b>Whole brain</b>						
Intercept	-0.315	0.038	-0.203	0.164	0.053	0.066
Slope	0.033	0.489	-0.007	0.097	-0.063	0.194
<b>Normalized thalamus</b>						
Intercept	-0.506	0.001	-0.973	<b>&lt;0.001</b>	-0.406	<b>&lt;0.001</b>
Slope	-0.647	<b>&lt;0.001</b>	-0.019	0.007	0.620	<b>&lt;0.001</b>
<b>Normalized caudate</b>						
Intercept	0.199	0.220	-0.113	0.382	-0.329	<b>&lt;0.001</b>
Slope	-0.563	<b>&lt;0.001</b>	-0.016	0.006	0.542	<b>&lt;0.001</b>
<b>Normalized putamen</b>						
Intercept	-0.281	0.076	-0.352	0.018	-0.076	0.044
Slope	-0.166	0.007	-0.001	0.913	0.184	0.004
<b>Normalized globus pallidus</b>						
Intercept	0.023	0.902	-0.524	0.002	-0.551	<b>&lt;0.001</b>
Slope	-0.528	<b>0.001</b>	-0.064	<b>&lt;0.001</b>	0.476	0.002

The accelerated decline in growth during the first year post-onset in thalamic, caudate, and globus pallidus volumes was observed only in children with MOGAD and brain lesions, while no significant differences between early and later follow-up could be documented among participants with normal brain MRI at presentation (eTable 3, [links.lww.com/WNL/C858](https://www.lww.com/WNL/C858)).

### Effect of Age at Onset and Presenting Phenotype on Growth Trajectories in Children With MOGAD

The inclusion of age at onset in the models did not reveal significant effects on the intercept or slopes of any of the structures examined (eTable 4, [links.lww.com/WNL/C858](https://www.lww.com/WNL/C858)). When assessing the growth trajectories in children with distinct phenotypes, both children with MOGAD presenting with ADEM (n = 15) and those presenting with monofocal ON (n = 21) showed reduced intercepts for normalized thalamic volumes and divergence from age-expected growth for thalamus, caudate, and globus pallidus. A direct comparison between the 2 groups did not show significant differences despite a tendency for steeper thalamic and putamen slopes in the ADEM group (eTable 5).

## Discussion

In this prospective cohort of children followed up from incident demyelinating episode for up to 12 years, we observed that MOGAD is associated with reduced age-expected growth

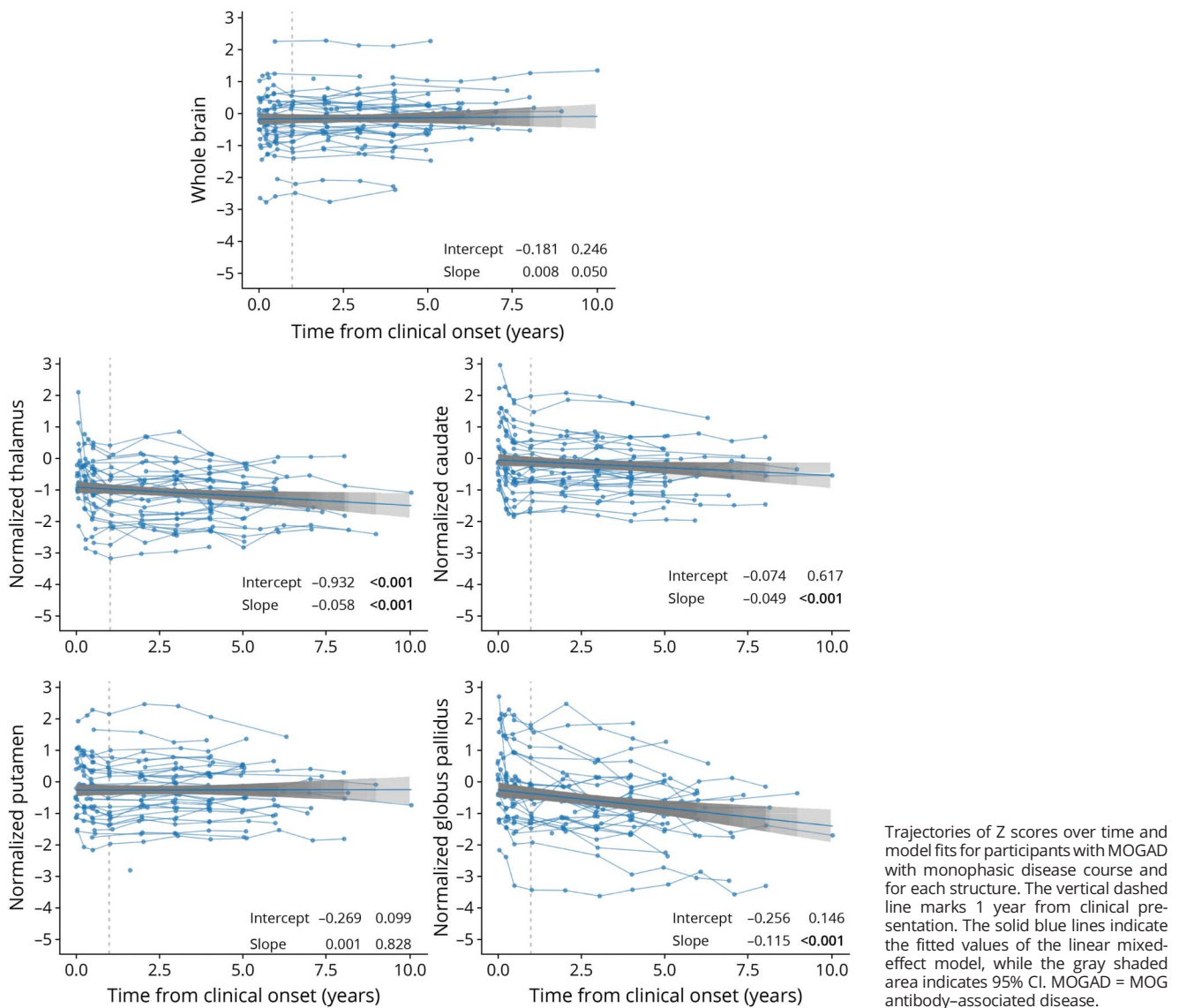
of multiple deep gray matter structures, disproportionately to the whole brain. Of note, we found a steeper divergence from the expected volume trajectories in the first year postonset, which was followed by a slower rate of progressive deviation from normal growth over the subsequent follow-up.

We also observed reduced cross-sectional Z scores at presentation with negative intercepts for normalized thalamic volume in children with MOGAD. While, on one hand, these findings might suggest that the onset of thalamic injury can even precede the incident clinical demyelinating event, on the other hand, they more likely could be explained by very rapid changes in thalamic volume in the first weeks after clinical presentation, resulting in negative values extrapolated at time zero. The median time from onset to first analyzed research MRI scan was 26 days, which while brief could conceptually be of sufficient duration as to have affected the linear extrapolations of volumes to time zero. Acquisition of research brain imaging was not always feasible on the days immediately after presentation when children were acutely ill, particularly given that sedation was not part of our research protocol.

We demonstrated impaired gray matter volume and growth even in patients with monophasic MOGAD, which aligns with previous studies showing that even a single attack of demyelination can impair maturational brain growth.<sup>6,13</sup> The observation of a steeper divergence from expected growth in the first year postonset suggests a disproportionate impact of the presenting attack on volume trajectories in children with



**Figure 3** Growth Trajectories in Children With Monophasic MOGAD



MOGAD. This concept of “attack-mediated brain insult” is consistent with the current observation that neurologic deficits in MOGAD are also closely linked to attacks and that neurologic deficits do not seem to accrue independent of relapses, in contrast to what is seen in MS. Brain volume loss might instead relate to retrograde and anterograde degeneration mediated by lesions in the white matter that then affect deep gray nuclei volume. In line with this hypothesis, white matter lesion load has been repeatedly associated with reduced brain volume in MS, particularly thalamic volume,<sup>5,35,36</sup> and has been associated with reduced gray matter volume in a recent cross-sectional study in adults with MOGAD.<sup>19</sup> Total T2 lesion volume has been shown to typically reduce dramatically over time in pediatric and adult MOGAD, which differs from the increasing accrual of new lesions and the limited regression of established lesions in MS.<sup>3,37</sup> Hence, we hypothesize that more direct attack-

mediated damage of gray matter structures and the WM pathways subserving them in MOGAD could contribute to the observed early acute injury and volume abnormalities, with a less injurious impact over time.

The magnitude of the longitudinal divergence of age-expected thalamic growth in children with MOGAD was 3.7 times smaller than the one measured in children with POMS and thus possibly associated with milder clinical correlates. Furthermore, patients with POMS experienced a more linear trajectory of divergence from expected thalamic growth compared with those with MOGAD, with differences becoming more noticeable at later follow-up points. This is consistent with ongoing disease activity at the tissue level, as evidenced by the chronic active lesions that are linked to progressive tissue injury in MS.<sup>38</sup> Such lesions do not appear to be characteristic of MOGAD,<sup>38</sup> although pathologic

**Table 4** Z Scores for MOGAD With and Without Brain Lesions at Presentation

	MOGAD with brain lesions, n = 34		MOGAD without brain lesions, n = 11		MOGAD with brain lesions vs MOGAD without brain lesions	
	Coef.	p Value	Coef.	p Value	Coef.	p Value
<b>Whole brain</b>						
Intercept	-0.183	0.169	-0.446	0.266	0.263	0.418
Slope	-0.006	0.094	-0.004	0.494	-0.001	0.846
<b>Normalized thalamus</b>						
Intercept	-0.956	<b>&lt;0.001</b>	-0.474	0.005	-0.482	0.097
Slope	-0.042	<b>&lt;0.001</b>	-0.017	0.119	-0.025	0.149
<b>Normalized caudate</b>						
Intercept	-0.016	0.916	0.225	0.408	0.209	0.491
Slope	-0.032	<b>&lt;0.001</b>	-0.020	0.044	-0.012	0.384
<b>Normalized putamen</b>						
Intercept	-0.431	0.010	-0.075	0.793	-0.355	0.289
Slope	-0.001	0.968	-0.005	0.561	0.005	0.619
<b>Normalized globus pallidus</b>						
Intercept	-0.421	0.021	-0.048	0.858	-0.468	0.189
Slope	-0.124	<b>&lt;0.001</b>	-0.081	<b>&lt;0.001</b>	-0.044	0.058

studies, particularly in children, are limited. Whole-brain volume trajectories were not significantly different between children with MOGAD and POMS. Of note, we detected an almost significant divergence from expected whole brain growth in children with MOGAD, which may have contributed minimizing the difference in trajectory compared with children with POMS, and the limited sample size of this study might have reduced the ability to accurately capture smaller volume differences.

While we expected that age at onset would influence growth trajectories, with younger age rendering a child more susceptible to disease-mediated impact, we did not find this association to be statistically significant, possibly due to the size of our sample. Larger studies are required to discern characteristics that enhance vulnerability or, conversely, support the resilience of brain development and clarify whether the overall younger age of children with MOGAD could contribute to a different outcome of brain volume abnormalities compared with children with MS.

An inherent challenge facing longitudinal and multisite cohort studies is the need for multiple MRI scanners. We addressed this important issue, with extensive efforts to model scanner effects and adjust for such contributions.<sup>26,33</sup> A second challenge in the study of pediatric MOGAD, POMS, and seronegative mono-ADS is the rarity of these illnesses in children, which results in a relatively small number of study participants. Thus, for example, few children with MOGAD in our

cohort had a relapsing disease course, and the demographic and clinical features of these relapsing patients were skewed toward older age at onset and more frequent presentation with monofocal ON (which are recognized characteristics of relapsing MOGAD). For these reasons, we believed that our study cohort was underpowered to formally compare the growth trajectories of children with monophasic vs relapsing disease. International collaborative studies are required to further elucidate the precise impact of multiple episodes of demyelination on brain development and their implications for long-term clinical outcomes, and one hopes that efforts to establish methods for comparative analytics of MRI scans obtained on scanners by different manufacturers and of scans acquired at different field strengths will permit such multisite efforts.

In conclusion, we demonstrate the negative impact on brain development of even a single episode of demyelination in a cohort of children with MOGAD. Future collaborative efforts are needed to power more comprehensive analyses of different clinical presentations, age at onset, and relapsing vs monophasic courses. Such studies should also assess the important topic of potential protective effects of acute and chronic therapies on brain maturation and growth.

### Study Funding

This study was funded by the Canadian Multiple Sclerosis Scientific Research Foundation (Drs Banwell, Yeh, Marrie,

Arnold, and Bar-Or) and by funding provided by the Children's Hospital of Philadelphia. Dr. Waters is supported by NHS National Specialized Commissioning Group for Neuromyelitis Optica, UK. Dr. Marrie is supported by the Waugh Family Chair in Multiple Sclerosis.

## Disclosure

G. Fadda, A.C. de la Parra, and J. O'Mahony report no disclosures relevant to the manuscript; P. Waters and the University of Oxford hold patents for antibody assays and receive royalties, he has received speaker honoraria from Alexion, Roche, and UBC, he is codirector of Oxford Autoimmune Diagnostic Laboratory where MOG antibody testing is performed; E.A. Yeh reports personal fees for consulting from Biogen, Hoffmann-Laroché, and Alexion; grants from Biogen, Ontario Institute for Regenerative Medicine, Stem Cell Network, Center for Brain and Mental Health, The Peterson Foundation, National MS Society, MS Scientific Foundation, NIH, and Canadian Institutes of Health Research and Consortium of MS Centers; ABO participated as a speaker in meetings sponsored by and received consulting fees and/or grant support from: Janssen/Actelion; Atara Biotherapeutics, Biogen Idec, Celgene/Receptos, Roche/Genentech, Medimmune, Merck/EMD Serono, Novartis, and Sanofi-Genzyme; R.A. Marrie receives research funding from: CIHR, Research Manitoba, Multiple Sclerosis Society of Canada, Multiple Sclerosis Scientific Foundation, Crohn's and Colitis Canada, National Multiple Sclerosis Society, CMSC, and The Arthritis Society, and she is supported by the Waugh Family Chair in Multiple Sclerosis; S. Narayanan has received research funding from the Canadian Institutes of Health Research, the International Progressive MS Alliance, the Myelin Repair Foundation and Immunotec, honoraria/travel support from Genentech and MedDay, and personal compensation from NeuroRx Research; DLA reports personal fees for consulting from Acorda, Biogen, Celgene, F. Hoffmann-La Roche, Frequency Therapeutics, GeNeuro, MedImmune, Merck-Serono, Novartis, and Sanofi-Aventis, grants from Biogen, Immunotec, and Novartis, and equity interest in NeuroRx Research; D.L. Collins reports grants from Canadian Institute of Health Research, during the conduct of the study, and personal fees from NeuroRx Inc., outside the submitted work; B. Banwell receives funding from the Multiple Sclerosis Scientific Foundation and the National Multiple Sclerosis Society, she has received consultancy fees from Novartis, UCB pharmaceuticals, and Medscape, and she serves as a nonremunerated advisor on clinical trial design for Novartis, Biogen, Teva Neuroscience, Roche, and Sanofi-Aventis. Go to [Neurology.org/N](https://www.neurology.org/N) for full disclosures.

## Publication History

Received by *Neurology* November 26, 2022. Accepted in final form April 4, 2023. Submitted and externally peer reviewed. The handling editor was Associate Editor Courtney Wusthoff, MD, MS.

## Appendix 1 Authors

Name	Location	Contribution
<b>Giulia Fadda, MD</b>	Department of Medicine, University of Ottawa, Ottawa Hospital Research Institute	Drafting/revision of the article for content, including medical writing for content; study concept or design; and analysis or interpretation of data
<b>Alonso Cardenas de la Parra, PhD</b>	Montreal Neurological Institute, McGill University, Quebec, Canada	Drafting/revision of the article for content, including medical writing for content; analysis or interpretation of data
<b>Julia O'Mahony, PhD</b>	Department of Community Health Sciences, Max Rady College of Medicine, Rady Faculty of Health Sciences, University of Manitoba, Winnipeg, Canada	Drafting/revision of the article for content, including medical writing for content
<b>Patrick Waters, PhD</b>	Nuffield Department of Clinical Neurosciences, John Radcliffe Hospital, University of Oxford, United Kingdom	Drafting/revision of the article for content, including medical writing for content; major role in the acquisition of data; and analysis or interpretation of data
<b>E. Ann Yeh, MD</b>	Department of Pediatrics, University of Toronto, Ontario, Canada	Drafting/revision of the article for content, including medical writing for content; major role in the acquisition of data
<b>Amit Bar-Or, MD</b>	Center for Neuroinflammation and Neurotherapeutics, and Department of Neurology, Perelman School of Medicine, University of Pennsylvania, Philadelphia	Drafting/revision of the article for content, including medical writing for content; major role in the acquisition of data
<b>Ruth Ann Marrie, MD, PhD</b>	Department of Community Health Sciences and Department of Internal Medicine, Max Rady College of Medicine, Rady Faculty of Health Sciences, University of Manitoba, Winnipeg, Canada	Drafting/revision of the article for content, including medical writing for content; major role in the acquisition of data
<b>Sridar Narayanan, PhD</b>	Montreal Neurological Institute, McGill University, Quebec, Canada	Drafting/revision of the article for content, including medical writing for content
<b>Douglas L. Arnold, MD</b>	Montreal Neurological Institute, McGill University, Quebec, Canada	Drafting/revision of the article for content, including medical writing for content; major role in the acquisition of data
<b>D. Louis Collins, PhD</b>	Montreal Neurological Institute, McGill University, Quebec, Canada	Drafting/revision of the article for content, including medical writing for content; study concept or design; and analysis or interpretation of data
<b>Brenda Banwell, MD</b>	Division of Child Neurology, Department of Neurology, The Children's Hospital of Philadelphia, Perelman School of Medicine, University of Pennsylvania	Drafting/revision of the article for content, including medical writing for content; major role in the acquisition of data; study concept or design; and analysis or interpretation of data

## Appendix 2 Coinvestigators

Name	Location	Role	Contribution
<b>Mark Awuku, MD</b>	University of Windsor, Windsor, Ontario, Canada	Subsite investigator	Enrollment and follow-up of study participants
<b>J. Burke Baird, MD</b>	McMaster University, Hamilton, Ontario, Canada	subsite investigator	Enrollment and follow-up of study participants
<b>Virender Bhan, MD</b>	Dalhousie University, Halifax, Nova Scotia, Canada	subsite investigator	Enrollment and follow-up of study participants
<b>David Buckley, MD</b>	Janeway Children's Health and Rehabilitation Centre, St John's, Newfoundland and Labrador, Canada	subsite investigator	Enrollment and follow-up of study participants
<b>David Callen, MD</b>	Hamilton Health Sciences Center, Hamilton, Ontario, Canada	subsite investigator	Enrollment and follow-up of study participants
<b>Mary B. Connolly, MBBCh</b>	Children's Hospital of British Columbia, Vancouver, British Columbia, Canada	subsite investigator	Enrollment and follow-up of study participants
<b>Marie-Emmanuelle Dilenge, MD</b>	Montreal Children's Hospital, Montreal, Quebec, Canada	subsite investigator	Enrollment and follow-up of study participants
<b>Asif Doja, MD</b>	Children's Hospital of Eastern Ontario, Ottawa, Ontario, Canada	subsite investigator	Enrollment and follow-up of study participants
<b>Simon Levin, MD</b>	University Hospital London, London, Ontario, Canada	subsite investigator	Enrollment and follow-up of study participants
<b>Anne Lortie, MD</b>	CHU Sainte-Justine, Montreal, Quebec, Canada	subsite investigator	Enrollment and follow-up of study participants
<b>E. Athen MacDonald, MD</b>	Hôtel-Dieu de Paris, Kingston, Ontario, Canada	subsite investigator	Enrollment and follow-up of study participants
<b>Jean K. Mah, MD</b>	Alberta Children's Hospital, Calgary, Alberta, Canada	subsite investigator	Enrollment and follow-up of study participants
<b>Brandon Meaney, MD</b>	Hamilton Health Sciences Center, Hamilton, Ontario, Canada	subsite investigator	Enrollment and follow-up of study participants
<b>David Meek, MD</b>	St John Regional Hospital Facility, St John, New Brunswick, Canada	subsite investigator	Enrollment and follow-up of study participants
<b>Daniela Pohl, MD</b>	Children's Hospital of Eastern Ontario, Ottawa, Ontario, Canada	subsite investigator	Enrollment and follow-up of study participants

## Appendix 2 (continued)

Name	Location	Role	Contribution
<b>Giillaume Sebire, MD</b>	Montreal Children's Hospital, Montreal, Quebec, Canada	subsite investigator	Enrollment and follow-up of study participants
<b>Sunita Venkateswaran, MD</b>	Children's Hospital of Eastern Ontario, Ottawa, Ontario, Canada	subsite investigator	Enrollment and follow-up of study participants
<b>Amy Waldman, MD</b>	Children's Hospital of Philadelphia, Philadelphia, Pennsylvania	subsite investigator	Enrollment and follow-up of study participants
<b>Katherine Wambara, MD</b>	Victoria General Hospital, Victoria, British Columbia, Canada	subsite investigator	Enrollment and follow-up of study participants
<b>Ellen Wood, MD</b>	Dalhousie University, Halifax, Nova Scotia, Canada	subsite investigator	Enrollment and follow-up of study participants
<b>Jerome Yager, MD</b>	Children's Stollery Hospital, Edmonton, Alberta, Canada	subsite investigator	Enrollment and follow-up of study participants

## References

- Fadda G, Armangue T, Hacothen Y, Chitnis T, Banwell B. Paediatric multiple sclerosis and antibody-associated demyelination: clinical, imaging, and biological considerations for diagnosis and care. *Lancet Neurol.* 2021;20(2):136-149. doi:10.1016/s1474-4422(20)30432-4
- Bruijstens AL, Lechner C, Flet-Berliac L, et al. E.U. paediatric MOG consortium consensus: part 1 - classification of clinical phenotypes of paediatric myelin oligodendrocyte glycoprotein antibody-associated disorders. *Eur J Paediatr Neurol.* 2020;29:2-13. doi:10.1016/j.ejpn.2020.10.006
- Waters P, Fadda G, Woodhall M, et al. Serial anti-myelin oligodendrocyte glycoprotein antibody analyses and outcomes in children with demyelinating syndromes. *JAMA Neurol.* 2020;77(1):82-93. doi:10.1001/jamaneurol.2019.2940
- Armangue T, Olive-Cirera G, Martinez-Hernandez E, et al. Associations of paediatric demyelinating and encephalitic syndromes with myelin oligodendrocyte glycoprotein antibodies: a multicentre observational study. *Lancet Neurol.* 2020;19(3):234-246. doi:10.1016/s1474-4422(19)30488-0
- De Meo E, Meani A, Muiola L, et al. Dynamic gray matter volume changes in pediatric multiple sclerosis: a 3.5 year MRI study. *Neurology.* 2019;92(15):e1709-e1723. doi:10.1212/wnl.00000000000007267
- Longoni G, Brown RA, MomayyezSiahkhal P, et al. White matter changes in paediatric multiple sclerosis and monophasic demyelinating disorders. *Brain.* 2017;140(5):1300-1315. doi:10.1093/brain/awx041
- Aubert-Broche B, Fonov V, Narayanan S, et al. Onset of multiple sclerosis before adulthood leads to failure of age-expected brain growth. *Neurology.* 2014;83(23):2140-2146. doi:10.1212/wnl.00000000000001045
- Bartels F, Nobis K, Cooper G, et al. Childhood multiple sclerosis is associated with reduced brain volumes at first clinical presentation and brain growth failure. *Mult Scler.* 2019;25(7):927-936. doi:10.1177/1352458519829698
- Cobo-Calvo A, Ruiz A, Rollot F, et al. Clinical features and risk of relapse in children and adults with myelin oligodendrocyte glycoprotein antibody-associated disease. *Ann Neurol.* 2020;89(1):30-41. doi:10.1002/ana.25909
- Hacothen Y, Wong YY, Lechner C, et al. Disease course and treatment responses in children with relapsing myelin oligodendrocyte glycoprotein antibody-associated disease. *JAMA Neurol.* 2018;75(4):478-487. doi:10.1001/jamaneurol.2017.4601
- Hennes EM, Baumann M, Schanda K, et al. Prognostic relevance of MOG antibodies in children with an acquired demyelinating syndrome. *Neurology.* 2017;89(9):900-908. doi:10.1212/wnl.00000000000004312
- Bruijstens AL, Breu M, Wendel EM, et al. E.U. paediatric MOG consortium consensus: part 4 - outcome of paediatric myelin oligodendrocyte glycoprotein antibody-associated disorders. *Eur J Paediatr Neurol.* 2020;29:32-40. doi:10.1016/j.ejpn.2020.10.007
- Aubert-Broche B, Weier K, Longoni G, et al. Monophasic demyelination reduces brain growth in children. *Neurology.* 2017;88(18):1744-1750. doi:10.1212/wnl.0000000000003884



14. Reindl M, Schanda K, Woodhall M, et al. International multicenter examination of MOG antibody assays. *Neurol Neuroimmunol Neuroinflamm*. 2020;7(2):e674. doi:10.1212/xxi.0000000000000674
15. Canto LN, Bosca SC, Vicente CA, et al. Brain atrophy in relapsing optic neuritis is associated with crion phenotype. *Front Neurol*. 2019;10:1157. doi:10.3389/fneur.2019.01157
16. Schmidt FA, Chien C, Kuchling J, et al. Differences in advanced magnetic resonance imaging in MOG-IgG and AQP4-IgG seropositive neuromyelitis optica spectrum disorders: a comparative study. *Front Neurol*. 2020;11:499910. doi:10.3389/fneur.2020.499910
17. Duan Y, Zhuo Z, Li H, et al. Brain structural alterations in MOG antibody diseases: a comparative study with AQP4 seropositive NMOSD and MS. *J Neurol Neurosurg Psychiatry*. 2021;92(7):709-716. doi:10.1136/jnnp-2020-324826
18. Rechtman A, Brill L, Zveik O, et al. Volumetric brain loss correlates with a relapsing MOGAD disease course. *Front Neurol*. 2022;13:867190. doi:10.3389/fneur.2022.867190
19. Messina S, Mariano R, Roca-Fernandez A, et al. Contrasting the brain imaging features of MOG-antibody disease, with AQP4-antibody NMOSD and multiple sclerosis. *Mult Scler*. 2021;28(2):217-227. doi:10.1177/13524585211018987
20. Banwell B, Bar-Or A, Arnold DL, et al. Clinical, environmental, and genetic determinants of multiple sclerosis in children with acute demyelination: a prospective national cohort study. *Lancet Neurol*. 2011;10(5):436-445. doi:10.1016/s1474-4422(11)70045-x
21. Thompson AJ, Banwell BL, Barkhof F, et al. Diagnosis of multiple sclerosis: 2017 revisions of the McDonald criteria. *Lancet Neurol*. 2018;17(2):162-173. doi:10.1016/s1474-4422(17)30470-2
22. O'Mahony J, Marrie RA, Laporte A, et al. Recovery from central nervous system acute demyelination in children. *Pediatrics*. 2015;136(1):e115-e123. doi:10.1542/peds.2015-0028
23. Evans AC, Brain Development Cooperative G. The NIH MRI study of normal brain development. *Neuroimage*. 2006;30(1):184-202. doi:10.1016/j.neuroimage.2005.09.068
24. Gur RC, Richard J, Calkins ME, et al. Age group and sex differences in performance on a computerized neurocognitive battery in children age 8-21. *Neuropsychology*. 2012;26(2):251-265. doi:10.1037/a0026712
25. Cardenas-de-la-Parra A, Lewis JD, Fonov VS, et al. A voxel-wise assessment of growth differences in infants developing autism spectrum disorder. *Neuroimage Clin*. 2021;29:102551. doi:10.1016/j.nicl.2020.102551
26. Cardenas-de-la-Parra A, Martin-Brevet S, Moreau C, et al. Developmental trajectories of neuroanatomical alterations associated with the 16p11.2 Copy Number Variations. *Neuroimage*. 2019;203:116155. doi:10.1016/j.neuroimage.2019.116155
27. Manjon JV, Coupe P, Marti-Bonmati L, Collins DL, Robles M. Adaptive non-local means denoising of MR images with spatially varying noise levels. *J Magn Reson Imaging*. 2010;31(1):192-203. doi:10.1002/jmri.22003
28. Tustison NJ, Avants BB, Cook PA, et al. N4ITK: improved N3 bias correction. *IEEE Trans Med Imaging* 2010;29(6):1310-1320. doi:10.1109/tmi.2010.2046908
29. Dadar M, Fonov VS, Collins DL, Alzheimer's Disease Neuroimaging Initiative. A comparison of publicly available linear MRI stereotaxic registration techniques. *Neuroimage*. 2018;174:191-200. doi:10.1016/j.neuroimage.2018.03.025
30. Eskildsen SF, Coupe P, Fonov V, et al. BEaST: brain extraction based on nonlocal segmentation technique. *Neuroimage*. 2012;59(3):2362-2373. doi:10.1016/j.neuroimage.2011.09.012
31. Avants BB, Epstein CL, Grossman M, Gee JC. Symmetric diffeomorphic image registration with cross-correlation: evaluating automated labeling of elderly and neurodegenerative brain. *Med Image Anal*. 2008;12(1):26-41. doi:10.1016/j.media.2007.06.004
32. Fonov V, Evans AC, Botteron K, Almli CR, McKinstry RC, Collins DL. Unbiased average age-appropriate atlases for pediatric studies. *Neuroimage*. 2011;54(1):313-327. doi:10.1016/j.neuroimage.2010.07.033
33. Cárdenas de la Parra A. *MRI-Based Morphometry During Neurodevelopment*. McGill University; 2020.
34. Seabold S, Perktold J. *Statsmodels: econometric and statistical modeling with python. Proceedings of the 9th Python in Science Conference*; 2010:61.
35. Henry RG, Shieh M, Amirbekian B, Chung S, Okuda DT, Pelletier D. Connecting white matter injury and thalamic atrophy in clinically isolated syndromes. *J Neurol Sci*. 2009;282(1-2):61-66. doi:10.1016/j.jns.2009.02.379
36. Arnold DL, Sprenger T, Bar-Or A, et al. Ocrelizumab reduces thalamic volume loss in patients with RMS and PPMS. *Mult Scler*. 2022;28(12):1927-1936. doi:10.1177/13524585221097561
37. Sechi E, Krecke KN, Messina SA, et al. Comparison of MRI lesion evolution in different central nervous system demyelinating disorders. *Neurology*. 2021;97(11):e1097-e1109. doi:10.1212/wnl.00000000000012467
38. Hoftberger R, Guo Y, Flanagan EP, et al. The pathology of central nervous system inflammatory demyelinating disease accompanying myelin oligodendrocyte glycoprotein autoantibody. *Acta Neuropathol*. 2020;139(5):875-892. doi:10.1007/s00401-020-02132-y